

## Rainfall Fields in Israel and Jordan and the Effect of Cloud Seeding on Them

DAVID SHARON

*Institute of Earth Sciences, The Hebrew University of Jerusalem, Israel*

(Manuscript received 21 July 1977, in final form 27 September 1977)

### ABSTRACT

Spatial correlation functions of daily rainfall were derived separately for various parts of the study area and for unseeded and seeded days. The structure of respective rainfall fields was studied by means of the relationship between the geometry of iso-correlation contours of daily rainfall and the average geometry and/or kinematics of cloud systems that produce the rainfall. Results were obtained on 1) the prevalent direction of storm movement over the study area and 2) the change in size of rainfall areas under varying conditions.

Evidence is presented of an average increase of about 10 km in the dimensions of rainfall areas on seeded days. It is suggested that expanded rainfall areas have a twofold effect on the augmentation of the total yield of individual storms: 1) an increase of point rainfall resulting from prolonged exposure to moving cloud systems, and 2) an increase in the area thus affected. Consequently, the increase in water yield of a storm over the entire area covered by it, may not be fully represented by point measurements.

In the regional context, a contraction of storm areas was found in the transition to the arid zone. It is suggested that the size of rainfall areas is one of the fundamental factors controlling regional variations of rainfall as well as variations resulting from cloud seeding.

### 1. Introduction

The size and shape of areas receiving rainfall on single days vary considerably from day to day and are difficult to delineate unambiguously owing to network insufficiency. Consequently, it is difficult to obtain a representation of rainfall areas through conventional methods. On the other hand, the size of rainfall areas has been found to be a useful parameter in the study of the causes of variations in precipitation totals observed under various atmospheric conditions.

An attempt has been made here to derive some general characteristics of daily rainfall areas in Israel and some neighboring regions with the use of correlation analysis. Results of the analysis served 1) to study the orientation and typical shape of rainfall areas in a given region, 2) to determine the effect of rainfall stimulation activity on the dimensions of rainfall areas, and 3) to identify variations in the dimensions of rainfall areas in the transition from Mediterranean to arid parts of the study area.

The significance of the study of rainfall areas lies in their being related to variations in rainfall duration and in total rainfall under given conditions. Thus, differences in the size of rainfall areas may at least partially account for regional variations of rainfall totals, and for rainfall augmentation resulting from cloud seeding.

### 2. The method

Simple correlation maps have been used in previous studies in connection with the design of rainfall networks (Hershfield, 1968; Stol, 1972; and others). Maps of this type describe the spatial pattern of correlation in respect to one centrally located point on the map. An example is shown in Fig. 1. Assuming homogeneity of rainfields in respect to the correlation function within a given region, a more efficient estimation of spatial correlation surfaces has been attempted by means of composite correlation maps (Sharon, 1974a). This approach has been adopted for the present study.

The method consists essentially of an analysis of spatial correlation functions obtained for a set of stations, the field of which is homogeneous. Following the formulation by Gandin (1965), the functions are obtained as follows: let  $\mathbf{a}_i$ , ( $i=1, 2, \dots, n$ ), represent a set of  $n$  stations in which 24 h rainfall  $P$  is being observed;  $r_{ij}$  denotes an estimate of the correlation coefficient  $\rho_{ij}$  of  $P$  between  $\mathbf{a}_i$  and  $\mathbf{a}_j$ . For  $n$  stations,  $\binom{n}{2}$  different  $r$  values are obtained. The field of  $P$  over the area considered is defined as homogeneous in respect to the  $\rho_{ij}$ , provided the  $\rho_{ij}$  do not depend on the specific points  $\mathbf{a}_i, \mathbf{a}_j$ , but only on their vectorial difference:

$$\mathbf{d}_{ij} = \mathbf{a}_j - \mathbf{a}_i. \quad (1)$$

Thus,  $\rho_{ij}$  becomes a function of only the distance  $d$  and direction  $\varphi$  between points, i.e.,

$$\rho_{ij} = \rho(\mathbf{d}_{ij}) = \rho(d, \varphi). \quad (2)$$

For a homogeneous field, the empirical values  $r_{ij}$  of the function obtained for a given set of stations are most comprehensively represented by plotting all  $r_{ij}$  values on a polar diagram, with respective coordinates  $(d_{ij}, \varphi_{ij})$ . For each  $r_{ij}$ , an identical value of  $r_{ji}$  appears on the diagram at the diametrically opposite point relative to the origin. Thus the diagram is symmetric with respect to the reflection through the origin, and contains a total of  $2\binom{n}{2} = n(n-1)$  points. Iso-correlation lines may be interpolated to bring out the empirical space-correlation surface as in Fig. 3. The result is in fact a *composite* correlation map, containing the entire information from all  $n$  simple correlation maps (such as that shown in Fig. 1) taken together.

The *a priori* assumed homogeneity of a field should become apparent on the composite map in a consistent spatial distribution of  $r$ -values with little scatter about an interpolated correlation surface.

The interpretation of the pattern of spatial correlation functions in terms of the geometry of rainfall areas has been dealt with in a few studies. Gringorten (1973) and Sharon (1972, 1974b) have shown that the shape and rate of decrease of the function with distance are indicative of the average extent of the area similarly affected by rainfall in individual storms. Thus, the farther away from a station the correlation remains above some value of  $r$ , the farther do rainfall areas extend in respective directions. Accordingly, in a non-isotropic field, the axis of minimum decrease of  $r$  corresponds to the main direction in which rainfall areas on the ground are elongated. Such correspondence has actually been observed by Huff and Shipp (1969) who have derived correlation maps for various rainfall types in Illinois and found the elongation of iso-correlation lines to correspond to the predominant direction of storm movement. Fig. 1 shows another case, in which the general direction of moving thunderstorms is correctly reflected on the correlation map.

The correlation-distance relationship has also been used to study the relative spatial uniformity or spottiness of rainfall (Sharon, 1972). Gringorten (1973) has used correlation functions in a study of the spatial extent of 24 h rainfall in New England.

Using the spatial correlation functions in the above sense, it may be difficult to refer to some specific value of  $r$  as being actually indicative of the exact extent of rainfall on the ground. It seems that any choice of  $r$  would be arbitrary. Therefore, dimensions of rainfall areas in the present study have been deduced from correlation functions not in absolute terms but relative to each other only, such as when various directions (as above) or different areas or "treatments" have been

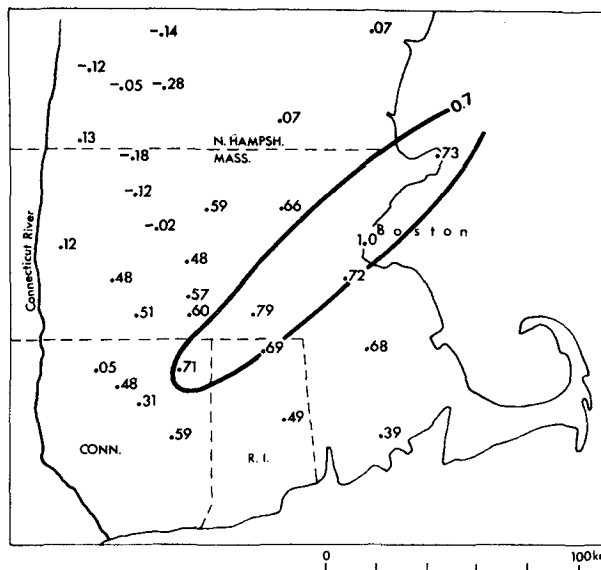


FIG. 1. A correlation map of daily rainfall totals on days with pronounced small-scale cellular convection in eastern Massachusetts, May–August 1962 and 1963. Correlation coefficients are all related to a single station (Boston). Raindays were included in the sample on the basis of radar observations, kindly made available by the Weather Radar Research Laboratory, MIT.

considered. The two latter cases will be further discussed in connection with respective results in Sections 5 and 6.

### 3. Data

Correlation coefficients  $r$  between 31 groups of stations in Israel, Jordan and Southern Lebanon have been calculated by Brier *et al.* (1974). Each group contained two to five stations located close to one another. This reduced noise in the data. Daily rainfall totals  $p$  obtained from the station groups, were transformed by Brier *et al.* (1974) into  $(p+1)^2$ , this transformation having been found by them to be more satisfactory for reducing the sampling variance of  $r$  than other ones. Transformations of this type may cause a general increase of  $r$  values, but their effect on the *pattern* of the iso-correlation lines is insignificant (Izawa, 1965). The increase of  $r$  values by itself does no harm in the present study, as reference will be made to *relative* values of  $r$  only, as already stated.

The present study focuses on 17 of the abovementioned station groups, located in hilly parts of the "central downwind area" in central Israel and part of the Kingdom of Jordan (Fig. 2). Mean annual rainfall in this area ranges from 300 to 600 mm. The rainfall field of all stations included has been found to be homogeneous in regard to the correlation function (see Fig. 3). The fact that local topography has no effect in this respect is not surprising, as topography-conditioned rainfall differences between points are persistent in time, and as such do not themselves affect the correlation function.

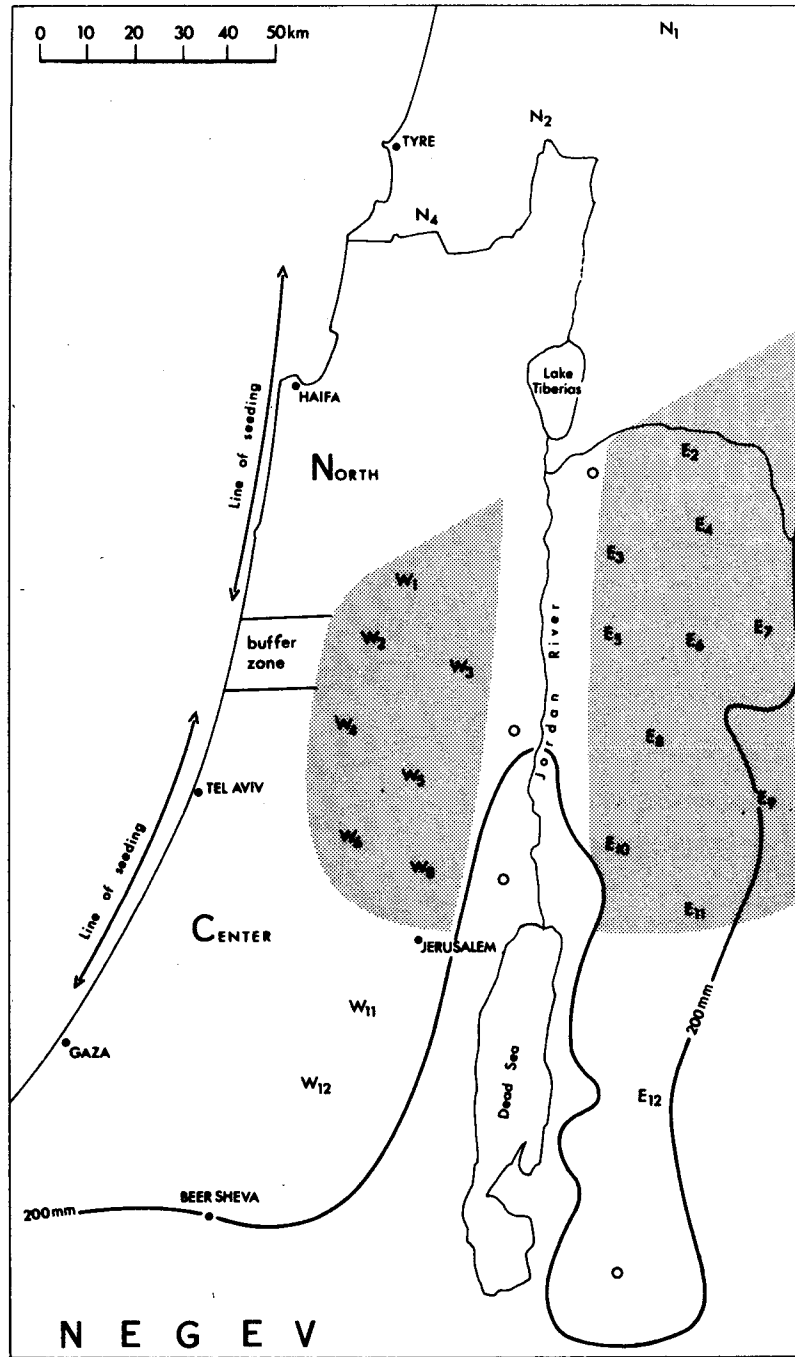


FIG. 2. The study area. The "central downwind area" is shown by stippling. W and E denote station groups. Small circles show the location of station groups not included in the analysis.

The 17 station groups in the central downwind area are evenly spread over the area. Therefore, all groups received the same weight in the analysis. Other station groups (shown in Fig. 2 north and south of the central area) have also been referred to in the study, in connection with the investigation of regional variations of correlation functions in Section 5.

Rainfall data of 275 days in 1960-67 have been used. During that period, a randomized crossover-precipitation augmentation experiment was in progress in Israel (Gagin and Neumann, 1974; Gabriel, 1970). On each day of the experiment, one of the two regions—North (N) or Center (C) in Fig. 2—was randomly chosen for seeding. Matrices of correlation coefficients were

derived separately for the 145 N-seeded and 130 C-seeded days.

According to the results obtained by Brier *et al.* (1974), all but three of the 17 station-groups treated here lie in the downwind area of C (Fig. 2). This area is essentially unaffected by cloud seeding on N-seeded days. The homogeneity of the field of *all* 17 stations implies that the three stations mentioned need not be excluded from this consideration. Consequently, Center- and North-seeded days of the experiment may justly be regarded as seeded and unseeded days, respectively, in relation to the central downwind area.

A presentation and discussion of results follows in Sections 4-6.

#### 4. The shape of the storm areas

The composite map on Fig. 3 shows the correlation

surface  $r(d, \varphi)$  of (nonseeded) daily rainfall in the central downwind area. It is based on  $\binom{17}{2} = 136$  different  $r$  values for each half of the area. The nonisotropy of the field is immediately apparent. Two distinct directions of frequent storm movement are indicated. The major axis is from an azimuth of  $235^\circ$  onto  $55^\circ$ . On rain days 500 and 700 mb winds are mostly from  $260-270^\circ$  (Gagin *et al.*, 1977), i.e., to the right of the above direction, similar to results in previous studies (Battan, 1973).

Farther downwind, the above axis curves to the left and assumes a more northerly direction. Apparently, this reflects a change in wind direction implied by the curvature of isobars around low-pressure centers, which are most frequently located northwest or north of the study area.

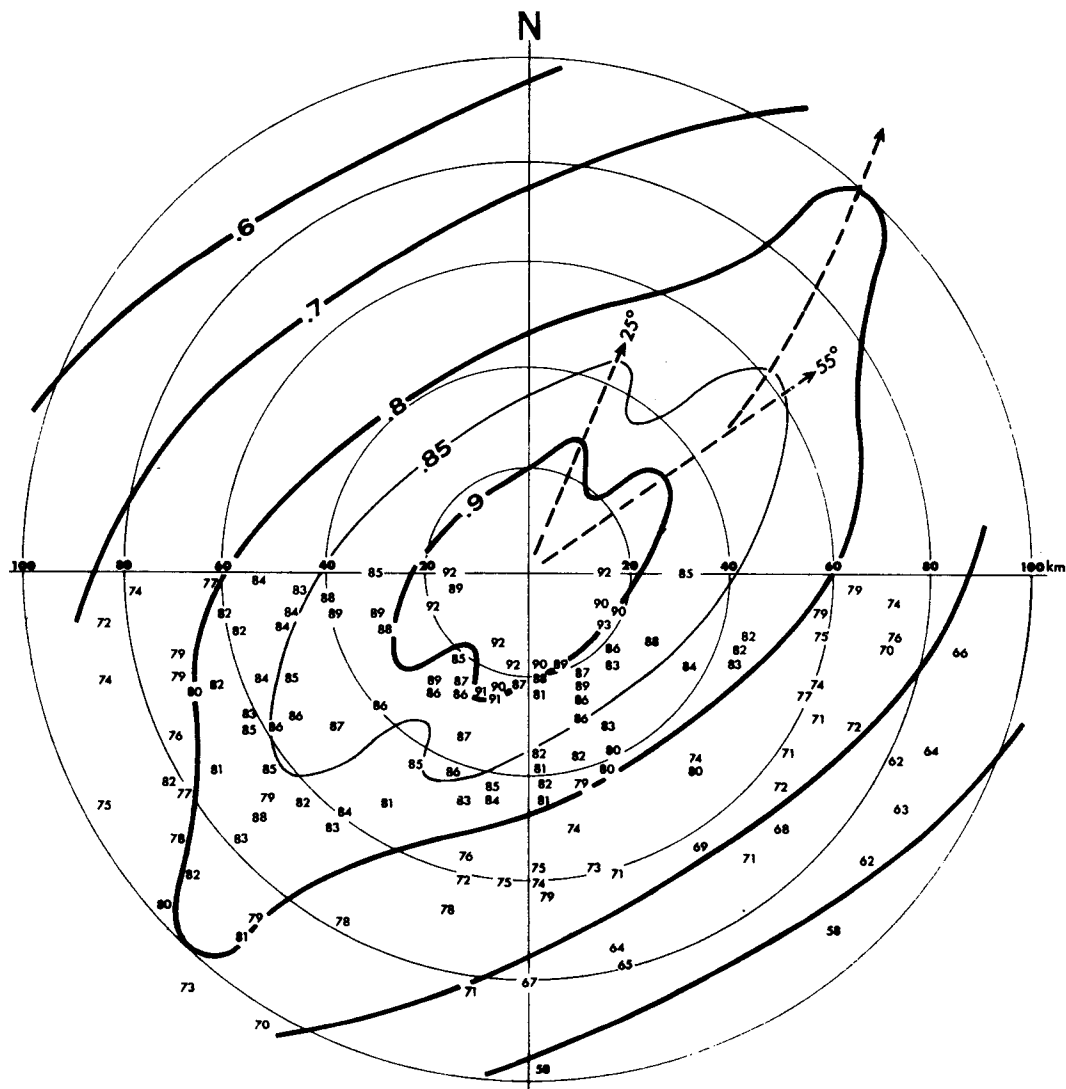


FIG. 3. Composite correlation map for all 17 station groups in the central downwind area shown in Fig. 2, nonseeded days. Isocorrelation lines are interpolated subjectively.

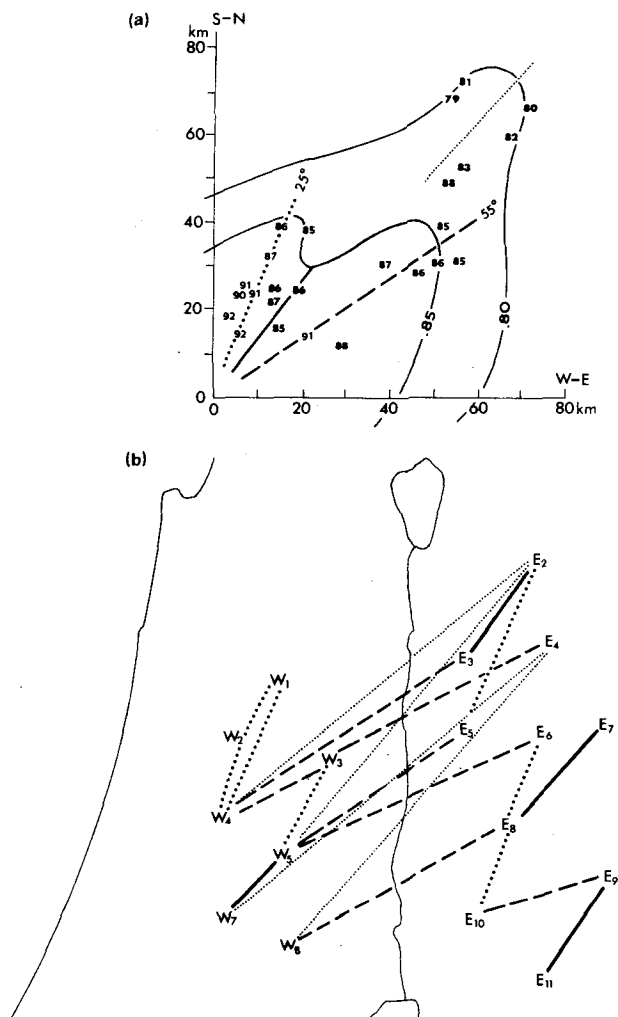


FIG. 4. Correlation coefficients along the main axes of storm movement. (a) Location on composite map as in Fig. 3; (b) geographical location of corresponding stations. The pairs of stations associated with each of the axes in (a) are connected in (b) by lines of the same type.

A secondary maximum at  $\phi = 25^\circ$  is also apparent up to a distance of 50 km beyond which it becomes diffuse. Fig. 4 shows that this is not merely an accidental result or one that represents some localized feature. The "decomposed" map in Fig. 4b shows the geographical location of the relatively high correlation coefficients associated with each of the two preferred directions, and also that of the lower coefficients lying in the intermediate direction. It may be seen that the values associated with each of the specified directions may be found throughout the entire area, wherever stations happen to be located in respective directions in relation to one another.

The physical nature of the secondary maximum is difficult to ascertain on the basis of existing information. It may reflect the orientation of less frequent storms, associated with the more southerly located

lows, off the coast near Gaza, or with the so-called Red Sea trough.

The relative dimensions of areas similarly affected by individual storms is shown in Figs. 3 and 5. Referring to any value of  $r$ , the downwind dimension is found to be about twice as large, on the average, as the width of the areas measured laterally at  $\phi = 145^\circ$ , across the main storm direction.

### 5. Regional variations of storm dimensions

Correlation functions for the area north and south of the central downwind area have been obtained, based on the correlation coefficients between the 17 stations dealt with above and two to three station groups north and south of that area, respectively. The stations in the north are  $N_1, N_2, N_4$  and in the south  $W_{11}$  and  $E_{12}$  (see Fig. 2). The resulting composite maps cover only a limited range of azimuths each; however, functions related to the width of areas could be derived from them, using  $r$  values at  $\phi = 145 \pm 20^\circ$  in the north and at  $145 \pm 30^\circ$  in the south. It should be noted that in all cases,  $r$  values pertain to the same 145 nonseeded days.

Resulting graphs in Fig. 6 show significant variations in rainfall areas. Thus, referring to any fixed-value of  $r$ , rainfall areas in the northern part of the country are by about 30 km wider than in the central part, whereas somewhat more to the south they measure by 20–25 km less.

The significance of regional variations in rainfall areas lies in the location of respective areas relative to the aridity line. The latter line is represented in Fig. 2 by the 200 mm (annual) isohyet. Viewing the above results in this context we find that the decrease in storm dimensions occurs in an area of diminishing rainfall, in the transition from a semi-arid Mediterranean climate in the north to the fringe of the arid zone in the south.

From the synoptic point of view, the above result reflects the difference in homogeneity of the rain-producing systems in the northern and southern parts of the area dealt with here. In the north, rain comes mostly from well-developed, homogeneous systems fed by the moisture-laden air flowing in from over the Mediterranean. Thus, continuous, extensive areas are covered by rain, producing large average rainfall areas.

In the south, on the other hand, a large part of the rainfall originates either 1) from peripheral, southward-extending parts of the above weather systems, which (owing to their peripheral position) are characterized by increased atmospheric stability or 2) from systems, the more southerly track of which increases the continental exposure of the incoming air. In both cases, the cloud cover is characteristically broken up into separate clusters and fragments, thus leading to a number of separate rainfall areas of smaller size. Hence, the diminishing size of rainfall areas from north to south reflects the transition from a predomi-

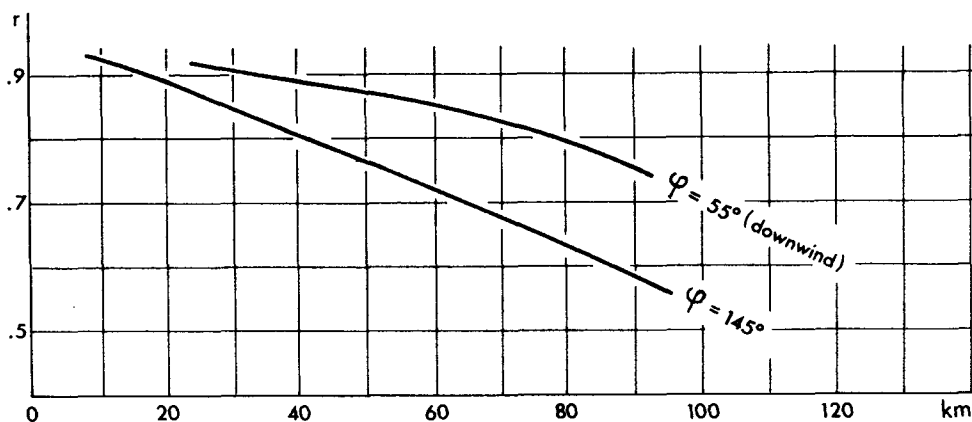


FIG. 5. Correlation functions in the directions of 55° and 145°, obtained from Fig. 3.

nance of more orderly, homogeneous rain-producing systems in the north, to an increasing proportion of scattered and localized showers typical of the more arid parts in the south.

Owing to the sparsity of stations in the Negev desert south of the 200 mm line, the present analysis could not be extended that far south. However, based on the relatively high frequency of local storms in the Negev, the average width of storm areas there is apparently even smaller. An example of small areas in a single event is shown in Fig. 7.

**6. Seeding effects**

The above results are all related to natural (non-seeded) conditions, since they have been obtained from data pertaining to the central area on North-seeded days. The same analysis has now been applied to seeded days, i.e., days on which the C-zone was seeded along a line lying offshore (see Fig. 2). The composite correlation map for seeded days is shown in Fig. 8 and

the distance-dependent function for  $\varphi=145^\circ$  derived from it in Fig. 9.

The results show that throughout the entire area, high-correlation values extend over larger areas on seeded days than on nonseeded ones. The difference between the two correlation surfaces should be viewed separately in the downwind direction and across it, at  $\varphi=145^\circ$ . In Fig. 9, the difference between distances corresponding to identical  $r$  values at  $\varphi=145^\circ$  is about 10 km. This reflects an expansion of the active parts of cloud systems, at least on a part of seeded days, such as a spreading out of rainfall on days on which otherwise it would have occurred in smaller areas only. It should be noted that this result applies to the study area in its entirety, extending almost 150 km downward from the line of seeding (see Fig. 2).

Referring to the physical nature of the regional changes in the structure of storms discussed in the preceding section, the increase in  $r$  values may also result from a change in the internal organization of

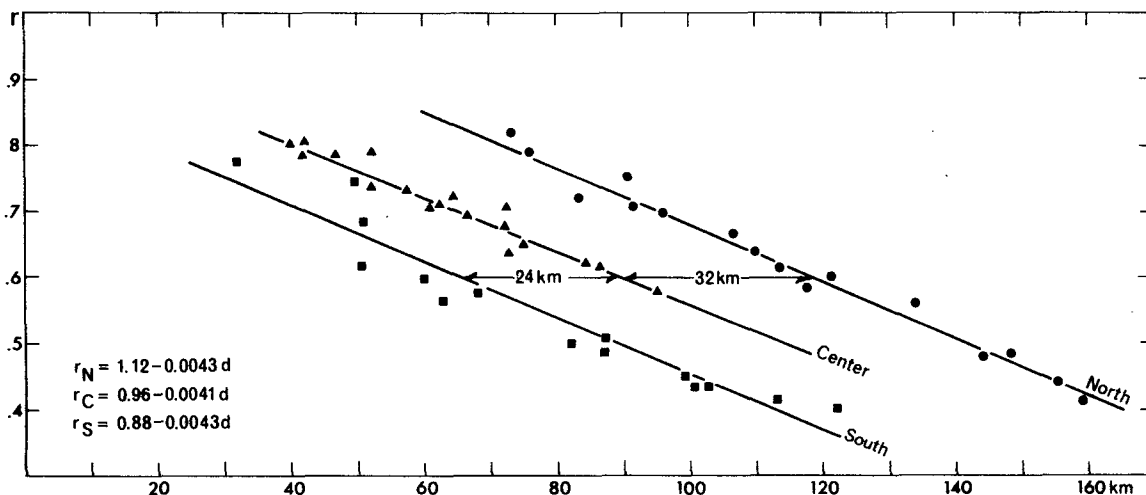


FIG. 6. Correlation functions at an azimuth of  $145^\circ \pm 20^\circ$  within the central downwind area, and between the central downwind area and stations north and south of it, respectively.

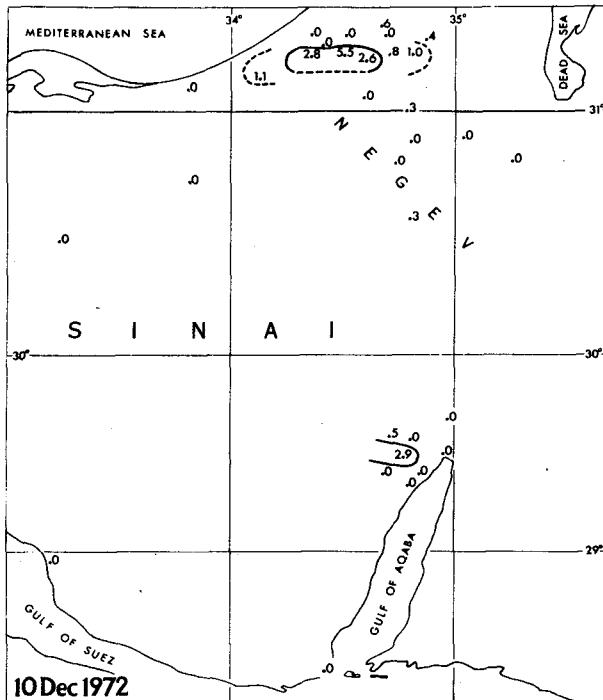


FIG. 7. Rainfall map for 10 December 1972. Rain amounts are given in mm. The scale may be determined by referring to the geographical coordinates.

systems, so that they are made more internally homogeneous. Theoretically, such change may occur in a given storm within original limits of rainfall areas with no corresponding expansion. This would imply that seeding causes a smoothing out of gaps existing within unseeded rain systems between distinct centers of activity. When a process of this kind occurs, it is likely to be especially effective at some distance away from the center of a system where gaps are pronounced, and it would lead to the merging of separate areas into larger ones. Hence, some expansion of the storm area is to be expected even in storms in which the increased spatial uniformity of rainfall may be the primary effect of seeding.

The width of rainfall systems in central Israel has been tentatively estimated from radar observations to be 65–82 km in most cases (Gagin *et al.*, 1977). An increase of 10 km would constitute 12–15%. On the basis of the consideration in the previous paragraph, the average increase in the width of rainfall areas may be somewhat lower, on the order of 10%.

To evaluate the above result, the change in rainfall areas should be viewed in context with other factors causing changes in total rainfall on seeded days, *viz.*, rainfall duration and intensity (Grant, 1976, personal communication). Referring to the Climax experiment conducted in Colorado, Chappell *et al.* (1971) have shown that “changes in the total precipitation are mainly controlled by changes in precipitation duration,

rather than intensity”. A 7–10% increase in duration, statistically significant at the very high level of  $\alpha = 0.7\%$ , has also been found recently in the Israeli experiment (Gagin and Neumann, 1976). In both cases, the results have been derived from recording raingages situated in respective study areas. This means that the durations considered represent the length of exposure of a fixed point on the ground to a system moving above it, and *not* the duration of the rain-producing process within the system itself. Now, for systems moving at a given speed, the length of exposure (i.e., the rainfall duration) is a function of the dimensions of the rainfall area of the system. It is worth noting here that the above-mentioned relative increase in the width of rainfall areas and in duration on seeded days actually is of the same magnitude. Hence, the increase in point rainfall that has been ascribed mainly to a prolonged *duration*, results—at least in part—from the expansion of rainfall *areas*. The change in rainfall areas that has been found in the present study, therefore, represents a fundamental effect of seeding that affects rainfall augmentation via rainfall duration.

## 7. Conclusions

The change in rainfall areas has been found in the present study to be a fundamental factor controlling regional variations of rainfall and variations resulting from cloud seeding.

In the regional context, this was deduced from the gradual contraction of rainfall areas that has been found in the transition from the relatively humid winters in the northern part of the study area to the more arid winters in the south. Regional differences of this kind are usually explained in terms of varying storm frequency, duration and intensity. It is suggested here, that although data on the size of rainfall areas are more difficult to obtain, it should certainly be considered among the basic parameters determining regional rainfall averages.

The expansion of rainfall areas on seeded days relative to nonseeded ones leads to a number of conclusions. First, it furnishes evidence for the validity of one of the underlying assumptions for the positive effects of seeding, namely, the postulate that the artificial introduction of ice crystals into certain types of cumulus clouds deficient of such precipitation embryos will result in the initiation of a rainfall process at points where otherwise it would not have formed naturally (Gagin and Neumann, 1974).

The concept of rainfall areas may also add to the already existing understanding of the effect of cloud seeding on rainfall augmentation. In a number of studies extended rainfall durations have been found on seeded days. These should be explained in terms of a prolonged exposure of points on the ground to expanded systems moving above them. Thus, the expansion of

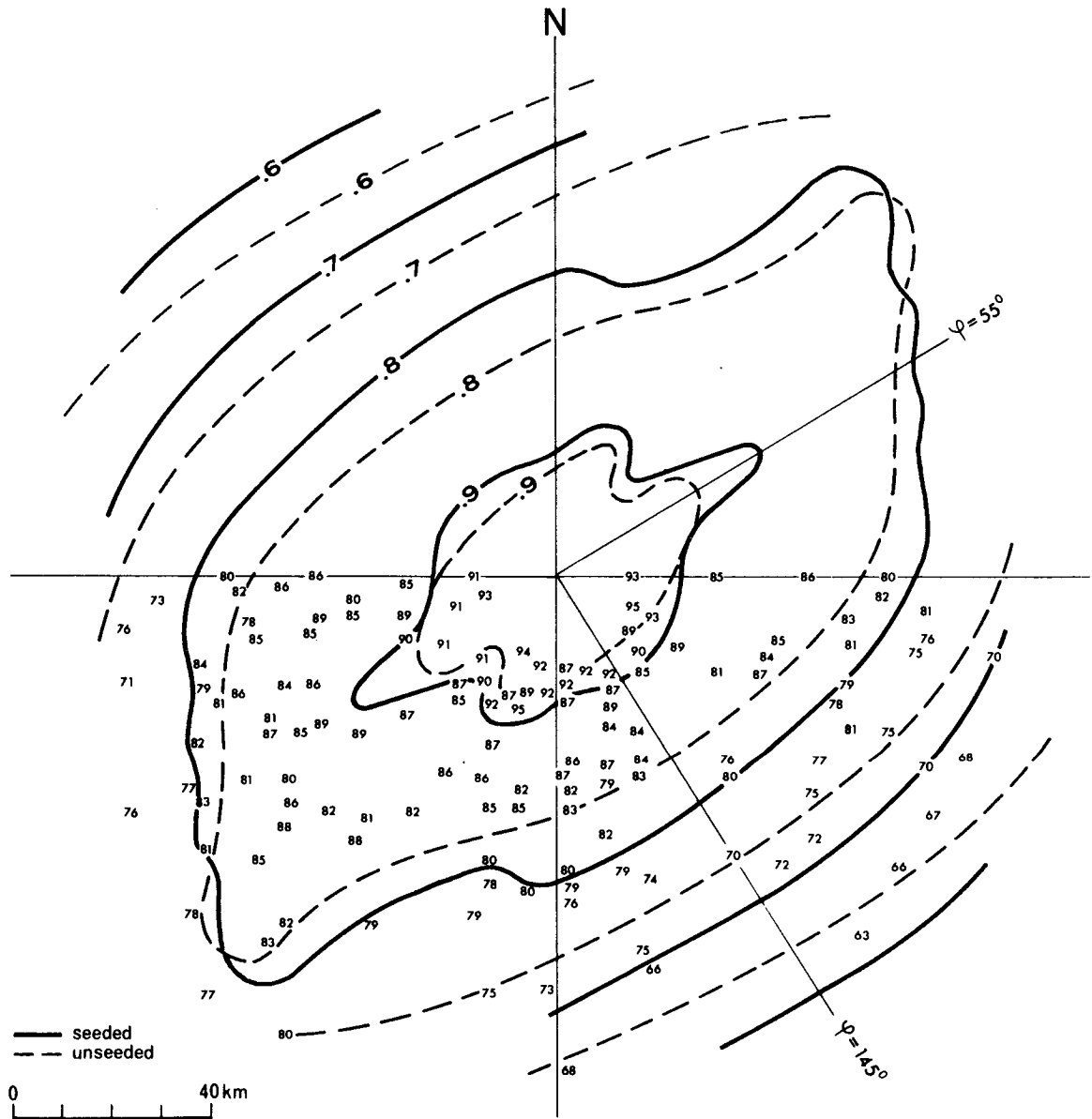


FIG. 8. Composite correlation map for the central downwind area, on seeded days. Isocorrelation lines for unseeded days (from Fig. 3) are also shown.

rainfall areas explains at least a part of the increased rainfall.

These conclusions lead to a reevaluation of the use of point rainfall as a measure of the effectiveness of rainfall stimulation. The changes in point rainfall and duration have often been used for this purpose. However, using the above concept, these parameters represent just a unidimensional expansion of rainfall areas, in the direction of storm movement only. They do not reflect the lateral dimension of rainfall areas, which is also affected on seeded days. Hence, the relative increase in gage catch may be smaller than the actual increase in the total volume of water yielded by a storm over its entire area. In other words, point rain-

fall, or even mean depth over relatively small areas, may not suffice for the full assessment of the effect of rainfall stimulation. A more adequate parameter for this purpose may be found by averaging storm rainfall over large areas, which is commensurate with the actual extent of expanded rainfall areas.

The last point may be illustrated in reference to the Israeli experiment. An increase of rainfall by 1.15 has been obtained as an areal average for the seeded region (Gagin and Neumann, 1976). Apparently, this reflects an approximate increase by  $(1.15)^3 = 1.07$  in point rainfall, which is in good agreement with the increase in duration and rainfall area mentioned above.



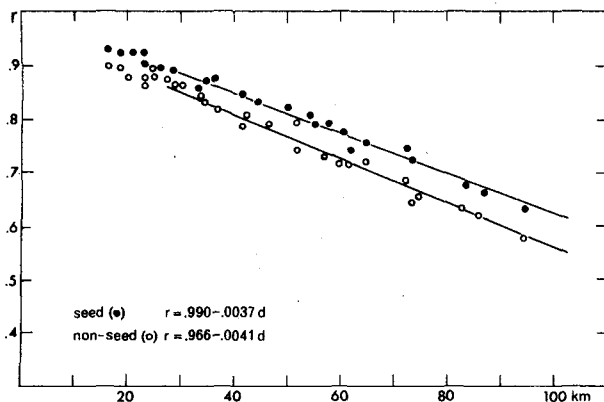


FIG. 9. Correlation functions in the direction of  $145^{\circ} \pm 25^{\circ}$  on seeded and unseeded days in the central downwind area.

*Acknowledgments.* A preliminary version of this paper has been presented at the Second Israeli Symposium on Physics of Clouds and of Precipitation Formation and Stimulation, Jerusalem 1975.

The author is indebted to Prof. L. O. Grant from the Department of Atmospheric Science, Colorado State University, and to Prof. J. Neumann and A. Gagin from the Department of Atmospheric Sciences, The Hebrew University of Jerusalem, for their encouragement and their most valuable suggestions on the manuscript. Additional constructive comments by Col. J. Barkan and D. Skibin are also gratefully acknowledged.

#### REFERENCES

Battan, L. J., 1973: *Radar Observation of the Atmosphere*, 2nd ed. The University of Chicago Press, 324 pp.

- Brier, G. W., L. O. Grant and P. W. Mielke, Jr., 1974: An evaluation of extended area effects from attempts to modify local clouds and cloud systems. *Proc. WMO/IAMAP Sci. Conf. on Weather Modification*, Tashkent, WMO No. 399, 439-448.
- Chappell, C. F., L. O. Grant and P. W. Mielke, Jr., 1971. Cloud seeding effects on precipitation intensity and duration on wintertime orographic clouds. *J. Appl. Meteor.*, **10**, 1006-1010.
- Gabriel, K. R., 1970: The Israeli rainmaking experiment 1961-67: Final statistical tables and evaluation. Hebrew University, Jerusalem, 47 pp.
- Gagin, A., and J. Neumann, 1974: Rain stimulation and cloud physics in Israel. *Weather and Climate Modification*, W. N. Hess, Ed., Wiley, 454-494.
- , and —, 1976: The second Israeli cloud seeding experiment—The effect of seeding on varying cloud populations. *Preprints 2nd WMO Conf. on Weather Modification*, Boulder, 195-204.
- , D. Rosenfeld and E. Hinkis, 1977: Unpublished reports.
- Gandin, L. S., 1965: *Objective Analysis of Meteorological Fields*. International Program Scientific Translations, Jerusalem.
- Gringorten, I. I., 1973: Stochastic modelling of the areal extent of weather conditions. AFCRL, Environ. Res. Pap. No. 459.
- Hershfield, D. M., 1968: Rainfall input for hydrological models. *Proc. Symp. Geochem., Precip., Evapor., Soil-Moisture, Hydrology*, Bern, Int. Assoc. Sci. Hydrol., Publ. No. 78, 177-188.
- Huff, F. A., and W. L. Shipp, 1969: Spatial correlations of storm, monthly and seasonal precipitation. *J. Appl. Meteor.*, **8**, 542-550.
- Izawa, T., 1965: Two or multi-dimensional Gamma-type distribution and its application to rainfall data. *Pap. Meteor. Geophys. Tokyo*, **15**, 167-200.
- Sharon, D., 1972: Spatial analysis of rainfall data from dense networks. *Hydrol. Sci. Bull.*, **17**, 291-300.
- , 1974a: The spatial pattern of convective rainfall in Sukumaland, Tanzania—A statistical analysis. *Arch. Meteor. Geophys. Bioklim.*, **B22**, 201-218.
- , 1974b: On the modelling of correlation functions for rainfall studies. *J. Hydrol.*, **22**, 219-224.
- Stol, P. T., 1972: The relative efficiency of the density of raingage networks. *J. Hydrol.*, **15**, 193-208.